J Mater Sci (2011) 46:1697–1704
DOI 10.1007/s10853-010-4987-1

The relationship of crystallization behavior, mechanical properties, and morphology of polypropylene nanocomposite fibers

Tawat Soitong · Jantrawan Pumchusak

Received: 3 August 2010 / Accepted: 6 October 2010 / Published online: 20 October 2010

Abstract This study aimed at the fabrication of lightweight and high performance nanocomposite fibers. Polypropylene/multiwalled carbon nanotubes (PP/MWCNTs) nanocomposite fibers (0–5 wt% of MWCNTs) were prepared via melt spinning process. The MWCNTs were dispersed in the dispersing agent before mixing with PP powder. After mixing, the dispersing agent was removed. Then the nanocomposites were spun into fibers. The fibers were spun and stretched with 7.5 draw ratios. Crystallization behavior and thermal properties of PP/MWCNTs nanocomposite fibers were studied using the differential scanning calorimeter (DSC) and thermogravimetric analyzer (TGA). The DSC curves of PP/MWCNTs nanocomposite fibers showed the crystallization peak at a temperature higher than that of neat PP fibers. These results revealed that the MWCNTs acted as nucleating sites for PP crystallization. The additions of MWCNTs into PP leaded to an increase in both crystallization temperature and crystallization enthalpy. However, no significant changes in the melting temperatures of the PP nanocomposites were detected. Degradation temperature of samples obtained from the TGA curves showed increase thermal degradation behavior for the PP/MWCNTs with the content of MWCNTs. It was found that the increase of tensile strength and modulus corresponded well with the increase of crystallinity of the composite fibers.

T. Soitong
Department of Physics and Materials Science,
Faculty of Science, NANOTEC Center of Excellence,
Chiang Mai University, Chiang Mai 50202, Thailand

J. Pumchusak (✉)
Department of Industrial Chemistry, Faculty of Science,
NANOTEC Center of Excellence, Chiang Mai University,
Chiang Mai 50202, Thailand
e-mail: jantrawan@gmail.com

Introduction

Carbon nanotubes (CNTs) (single-walled CNTs, double-walled CNTs, and multiwalled CNTs) were developed in 1990s [1, 2]. They have exceptional physical, mechanical, electrical, thermal, and optical properties [3, 4]. Significant breakthroughs have been reported in the processing of CNTs [5, 6] and their polymer nanocomposite films and fibers [7, 8]. CNTs have been used to reinforce many polymer matrix systems, including semi-crystalline and amorphous thermoplastics and thermosetting polymers [9–11].

Polypropylene (PP) is one of the most widely used polymers. Indeed, this polyolefin exhibits an attractive combination of low cost, lightweight, easy processing, and extraordinary versatility in terms of properties (it is known for its balance of strength, modulus, and chemical resistance). PP is found in many applications such as packaging, automotive industry, and fibers. This latter application had in recent years a rapid growth. This fiber was placed at the third rank of consumption of synthetic fibers, after polyester and polyamide fibers [12]. Several researches have used CNTs to improve the properties of the PP nanocomposites [13–17], they found that the CNTs enhanced the yield strength and Young's modulus of the nanocomposites. PP-based systems have been investigated on crystallization behavior and hence their crystal structures and polymorphic nature by several researchers [8, 18–21]. Non-isothermal crystallization studies on this system have shown that CNTs act as α-nucleating agents to create the α-crystal PP; therefore, CNTs do not influence the crystal

structure of the PP nanocomposite [8, 14, 15, 22]. Kim et al. [23] found that CNTs gave the better thermal stability to poly(ethylene 2,6-naphthalate). There were many studies showed that CNTs increased the degradation temperatures of the PP/CNTs nanocomposites [8, 15, 21, 22, 24].

Many researchers studied on the effect of multiwalled CNTs (MWCNTs) in PP nanocomposite on their properties [13, 14, 20, 21, 24]. However, a few of researches in nanocomposite fibers have been published [16, 17, 22]. In this work, the effects of different concentrations of MWCNTs on crystallization, thermal stability, and morphology of PP nanocomposite fibers had been investigated. In addition, the relation between the crystallization behavior and mechanical properties of fibers was explored.

Experimental

The PP used in this study was supplied by IRPC Public Co., Ltd., Thailand. It has a melt flow index of 11 g/10 min and $\overline{M_W}$ of 120,000 g/mol. MWCNTs was purchased from Nanomaterials Research Unit, Chiang Mai University, Thailand. The nanotubes have a diameter about 20–50 nm and a length of 10 μm [25]. SEM and TEM images of the MWCNTs are shown in Fig. 1a and b, respectively. The MWCNTs was calcined at 480 °C for 4 h prior to use in order to remove the amorphous carbon.

Dispersing agent is used to facilitate the dispersion of MWCNTs in PP matrix. In our previous study [26], sodium lauryl sulfate, Triton X-100 and 2-propanol were used as dispersing agents to disperse the MWCNTs in PP matrix, and tensile property of composite fibers was investigated. It was found that 2-propanol gave composite fibers with a better tensile property than other dispersing agents. Thus, in this study 2-propanol was selected to use as a dispersing agent. The 1 wt% MWCNTs were vibrated in 20 mL of 2-propanol with McCrone Micronizing Mill (McCrone, USA) for 1 h. PP powder was added to the solution and mixed by mechanical stirrer (Digital, IKA Group, Germany). Then the sample was dried at 70 °C in a vacuum oven about 2 h (samples were weighed until stable) and melt-blended using a two-rolls mixer at 190 °C for 20 min. After that, the nanocomposite fibers were spun using a home-made melt spinning equipment with a die diameter of 1.0 mm at 190 °C followed by a collection of the fiber on a speed take up device. The fibers were subsequently drawn at a draw ratio of 7.5 on a hot plate at 130 °C. Please note that the draw ratio is defined as the length of fiber after stretching divided by the original fiber length [27].

Non-isothermal crystallization analysis was performed by means of a differential scanning calorimeter (DSC, Instrument-specialists DSC 550, USA). The procedure performed in scans was the following; samples of about 10 mg were heated from 30 to 200 °C at a scan rate of 20 °C/min and the samples were cooled down to 30 °C using scan rates of 10 °C/min under nitrogen gas (20 mL/min) to obtain the melting and crystallization temperatures of nanocomposite fibers. The DSC analysis was performed twice for each fiber to confirm the results and to earn the average values. Heat of fusion was obtained by integration of the melting peak for the area under peak. The crystalline forming and its morphology of the neat PP and PP/1 wt% MWCNTs composite were studied on the thin films. Samples were melted and squeezed between glass slides to form the thin films at 200 °C and then cooled down to 130 °C with the cooling rate of 2 °C/min. The low cooling rate was used in order to allow the crystallization to take place [28]. Then the samples were quenched in liquid nitrogen in order to stop the crystal growth. After that, the crystalline morphology was observed under the optical polarizing microscope (Nikon eclipse E200, Thailand). Thermal stability of nanocomposite fibers was studied using thermogravimetric analyzer (TA Instruments, TGA 7, USA), and the scans were conducted under N_2 at a scan rate of 20 °C/min. Wide-angle X-ray diffraction spectra (XRD) of fibers were recorded with X'Pert MPD (multi-purpose diffraction, Phillips, The Netherlands); the X-ray beam was nickel-filtered Cu Kα radiation. Corresponding

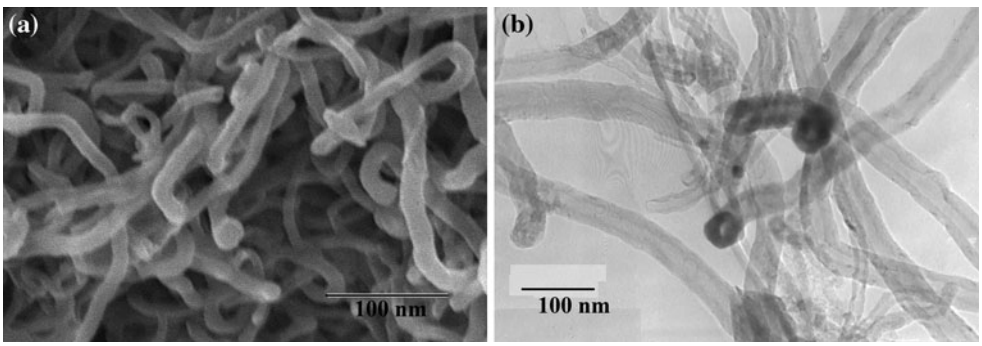

Fig. 1 **a** SEM image and **b** TEM image of MWCNTs after calcinations at 480 °C for 4 h

data were collected from 10° to 60° at a scanning rate of 3°/min.

Measurements of stress–strain curves of the nanocomposite fibers were performed using the LRX tensile tester (Lloyd Instruments, UK). A gauge length and a crosshead speed for the tensile tests were 30 mm and 30 mm/min, respectively [16]. The data were analyzed by using Duncan test of the analysis of variance (ANOVA). Mean values were considered at 95% significance level ($p < 0.05$). The morphology of the fibers was characterized by using scanning electron microscopy (SEM, JEOL JSM-6335F, Japan). The samples were prepared by fixing the samples on the stub then dipping it in liquid nitrogen and cutting them to reveal the cross-section. The samples were coated by gold before subjected to SEM. Transmission electron microscopy (TEM, JEOL JEM-2010, Japan), at an acceleration voltage of 85 kV was utilized to observe the axial sections of the samples. The samples were prepared by mounting the specimen with an epoxy resin and using a microtome (RMC, USA) to cut the samples with a thickness of 100–120 nm.

Results and discussion

Non-isothermal crystallization behavior

Figure 2 shows DSC thermograms of neat PP and PP/MWCNTs nanocomposite fibers at a heating and cooling rate of 10 °C/min. The melting temperature (T_m), the heat of fusion (ΔH_f), and the crystallization temperature (T_c) obtained from the DSC studies are summarized in Table 1. In order to estimate the percentage of crystallinity (χ), the following equation was used [13, 29];

$$\chi = \frac{\Delta H_f}{(1 - \phi_p) \times \Delta H_f^0} \times 100$$

where ϕ_p is the weight fraction of filler in the composite, ΔH_f is the heat of fusion of the analyzed sample (J/g), and ΔH_f^0 is a reference value that represents the heat of fusion for a 100% crystalline polymer. For PP, ΔH_f^0 is 209 J/g [30].

It can be seen that the melting temperature of PP/MWCNTs nanocomposite fibers did not change significantly compared to that of the neat PP fiber. Apparently, PP and PP/MWCNTs fibers showed the onset of melting temperature at about 156 °C. However, the multiple distinct melting peaks were observed (Fig. 2a) because of the difference of crystal forms or degree of perfection [31]. These kinds of peaks were found in fibers with high speed winding up, the higher the speed, the sharper the multiple peaks [32]. These peaks are related to transformations from folded-chain to extended-chain crystals [33]. It has been reported that carbon nanofibers in polyethylene nanocomposite fibers hinder the extended-chain crystal transformations, so the multiple sharp melting peaks were obscure [33]. In Fig. 2a, 5 wt% MWCNTs nanocomposite fibers show the melting peaks with shoulder at lower side, while neat PP fibers reveal the sharp melting peaks. This is a result of MWCNTs restricting molecular mobility of the PP chains. The heat of fusion of the PP nanocomposite fibers was increased when the content of MWCNTs increased. The results confirmed that the MWCNTs could increase the percentage of crystallinity. This was also reported by other researches [8, 20, 22, 23, 34]. However, in some matrices nanotube acts as obstacles to crystallization [32, 35].

The crystallization peaks of PP/MWCNTs nanocomposite fibers are narrower than those of neat PP fiber. Narrower crystallization peaks would suggest a narrower crystallite size distribution in the PP/MWCNTs nanocomposite fibers as compared to neat PP fiber. Ma et al. [36] also observed narrower crystallization peaks in polyethylene terephthalate/nanocarbon nanocomposite fiber as compared to neat polyethylene terephthalate fiber. The crystallization of PP/MWCNTs nanocomposite fibers began at a temperature higher than that of neat PP. Table 1 confirms the addition of MWCNTs in the PP matrix lead to an increase in the crystallization temperature. The relative shift of the T_c is gradual increased with content of MWCNTs. These results revealed that the MWCNTs act as nucleating agents for PP.

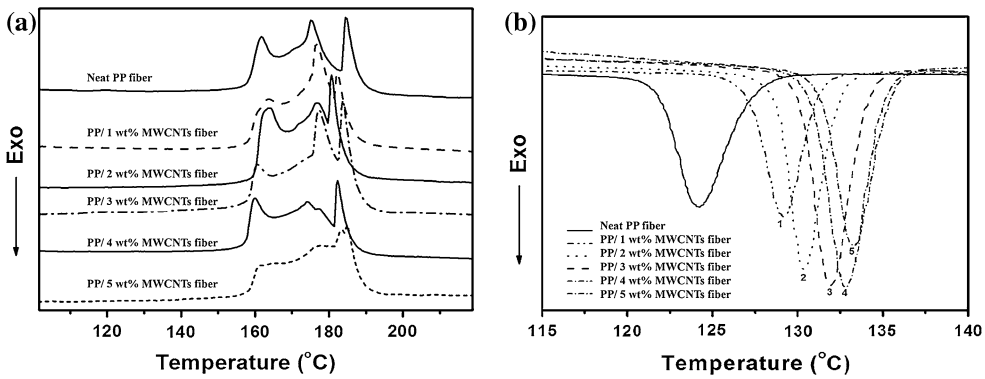

Fig. 2 DSC thermograms of the neat PP and PP/MWCNTs nanocomposite fibers with 1–5 wt% MWCNTs: **a** melting curves and **b** crystallization curves

Table 1 Thermal behavior of the neat PP and PP/MWCNTs nanocomposite fibers with 1–5 wt% MWCNTs

Composite fiber	T_m rang (°C)	ΔH_f (J/g of PP matrix)	T_c (°C)	ΔH_c (J/g of PP matrix)	χ_c (%)
Neat PP fiber	155.9–192.3	83.4	124.2	100.1	47.89
PP/1 wt% MWCNTs fiber	156.3–190.2	87.9	129.2	114.1	55.14
PP/2 wt% MWCNTs fiber	156.8–190.5	94.8	130.4	119.6	58.39
PP/3 wt% MWCNTs fiber	156.3–191.5	97.9	131.9	120.4	59.39
PP/4 wt% MWCNTs fiber	155.8–190.8	101.2	132.8	116.6	58.11
PP/5 wt% MWCNTs fiber	156.4–192.0	96.1	133.2	115.8	58.32

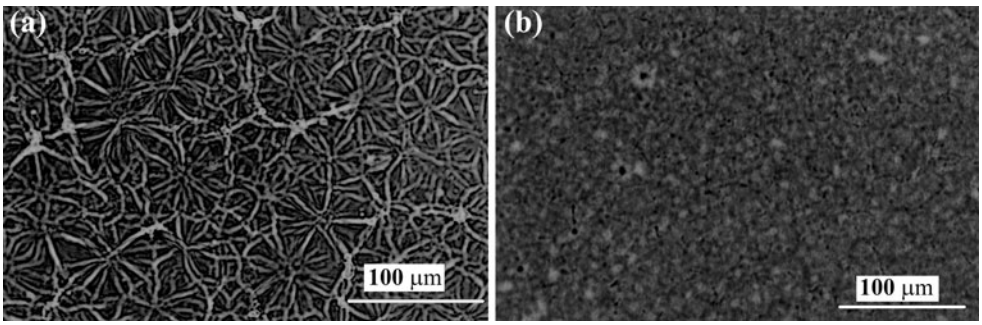

Fig. 3 Microphotographs of **a** neat PP and **b** PP/1 wt% MWCNTs nanocomposite

A similar nucleation effect has been found in the PP/SWCNTs [8, 19] and PP/MWCNTs nanocomposites [20]. Figure 3a and b shows the crystal micrographs of neat PP and 1 wt% nanocomposite, respectively. For the neat PP, large grains were observed. In the 1 wt% MWCNTs nanocomposites, a small crystal aggregates was visible. It was evident that the MWCNTs fillers refined the size of PP spherulites of the nanocomposite considerably, confirming that MWCNTs act as nucleating sites for PP crystallization. The nucleating agent enhances the crystallization rate and promotes the formation of intercrystalline links [37]. The intercrystalline links are bridges between and within spherulites generated by a PP chain that has one segment crystallized in a spherulite and another segment crystallized in another spherulite or another part of the same spherulite. Thus, a PP chain can "link" two spherulites together. A nucleating agent, through its ability to create intercrystalline links and smaller spherulites, improves the mechanical properties of the PP [37, 38].

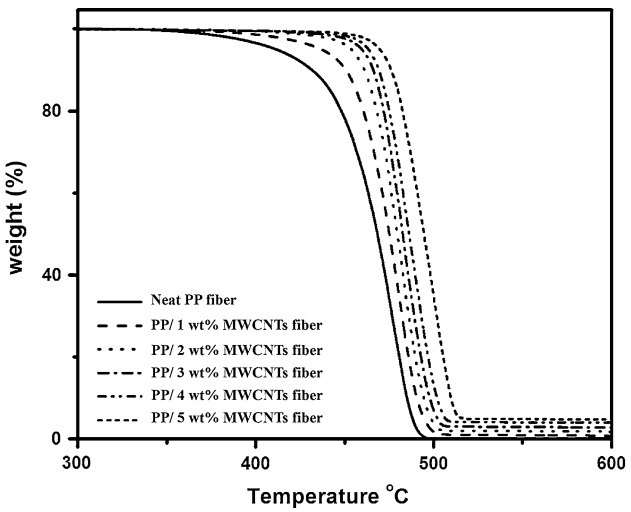

Fig. 4 TGA thermograms of the neat PP and PP/MWCNTs nanocomposite fibers with 1–5 wt% MWCNTs

Thermogravimetric analysis

A comparative TGA of neat PP and PP/MWCNTs nanocomposite fibers are shown in Fig. 4 and the corresponding data are given in Table 2. Figure 4 shows the shift of the onset of thermal degradation towards higher temperatures after introduction of the filler. The residual weight in the TGA study of PP/MWCNTs nanocomposite fibers in Fig. 4 at above 500 °C represented the weight of the MWCNTs in the nanocomposite. For the nanocomposite fibers with 1–5 wt% of MWCNTs, the onset of degradation temperatures were 40°–53° higher than that of the neat PP fiber. Similar trends have been reported by Bhattacharyya et al. [8] and Wang et al. [39] for PP/SWCNTs and PE/MWCNTs nanocomposite fibers, respectively. In addition, Jose et al. [22] reported an increase of 16° and 34° of the degradation temperatures of the PP/MWCNTs nanocomposites with the addition of 0.5 and 1 wt% of MWCNTs, respectively. The improvement in thermal stability can be attributed to good PP/MWCNTs interaction and also due to

the higher heat capacity of the MWCNTs [40] than that of PP matrix [41].

XRD analysis

The β-crystal PP melts at a temperature lower than the α-crystals for 12°–15° [42]. A melting temperature at about 165 °C in Table 1 is attributed to the melting of α-crystals in PP and PP/MWCNTs fibers. The X-ray diffraction of PP and the PP/MWCNTs nanocomposite fibers could confirm those results. The diffraction patterns for PP and PP/MWCNTs nanocomposite fibers are displayed in Fig. 5. The integrated X-ray diffraction intensity of PP and PP/MWCNTs nanocomposite fibers show the typical α-form PP crystals and exhibited complete absence of the β-crystal form. Neat PP fiber showed five prominent peaks in the 2θ in the range of 10°–30°, which correspond to the monoclinic α crystalline phase [21]. In the PP/MWCNTs nanocomposite fibers, the same number of peaks was observed in the same range of 2θ, which suggests that PP/MWCNTs nanocomposite fibers also contain mainly α-phase. This indicated that the addition of MWCNTs did not affect the crystalline structure of the PP matrix in this case. A similar behavior has been reported by other researchers [13, 15, 20, 38]. However, there is a difference in the relative intensities of the peaks for neat PP and PP/MWCNTs nanocomposite fibers. When the content of MWCNTs increased (1–3 wt%), the intensity of the peak of 2θ at 16.9° increased, while that of 2θ at 14.1° decreased. However, the intensity of the two peaks stayed stable when the content of MWCNTs increased from 3 to 5 wt%. Similar to the study of Lihua and Jing [43], they found an increase of the peak intensity at the same 2θ when added nanoclay into PP matrix. The crystallinity results from XRD corresponded well with the DSC analysis. The DSC results in Table 1 show an increase of the percentage of crystallinity with the increase of MWCNTs content at 1–3 wt%, while at 4–5 wt% no further increase in crystallinity is observed.

Table 2 Effect of MWCNTs on decomposition temperature of PP

Composite fiber	T_{onset} (°C)	T_{final} (°C)	Residual weight (%)
Neat PP fiber	302.76	507.01	0
PP/1 wt% MWCNTs fiber	355.17	517.69	1.016
PP/2 wt% MWCNTs fiber	345.77	513.67	1.994
PP/3 wt% MWCNTs fiber	345.96	516.17	3.006
PP/4 wt% MWCNTs fiber	342.32	525.23	4.108
PP/5 wt% MWCNTs fiber	341.26	537.43	4.894

Tensile properties and morphology

The stress–strain curves of neat PP fiber and PP nanocomposite fibers are shown in Fig. 6. Tensile strength and modulus values for neat PP fiber and the PP nanocomposite fibers are shown in Fig. 7. The MWCNTs in PP/MWCNTs nanocomposite fibers showed positive effect on mechanical properties. The tensile modulus was significantly increased with the increase of MWCNTs. The testing data showed an increase in the tensile modulus by 69, 71, 81, 90, and 84% for the 1, 2, 3, 4, and 5 wt% MWCNTs, respectively. Both tensile strength and modulus significantly increased when 1 wt% of MWCNTs was used. However, for the further increase of the content of MWCNTs (2–4 wt%), the improvement of these properties was declined. The tensile

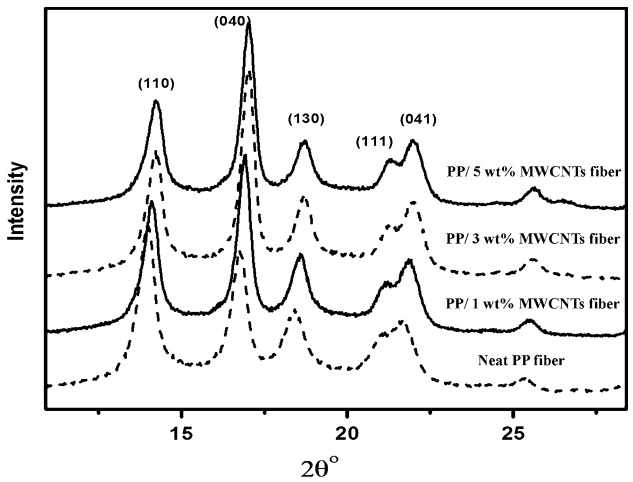

Fig. 5 XRD curves of the neat PP and PP/MWCNTs nanocomposite fibers with 1–5 wt% MWCNTs

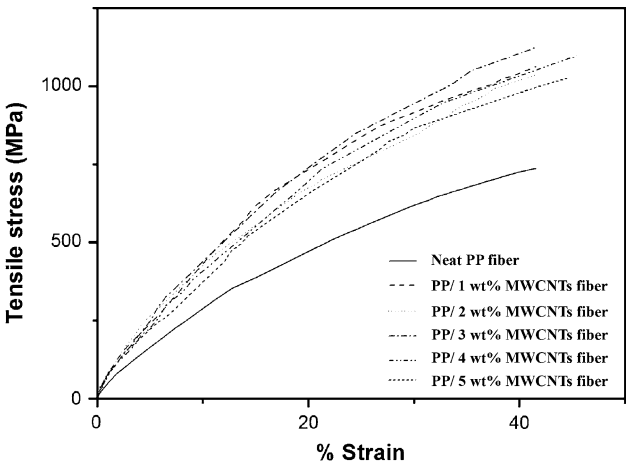

Fig. 6 Stress–strain curves of neat PP and PP/MWCNTs nanocomposite fibers with 1–5 wt% MWCNTs

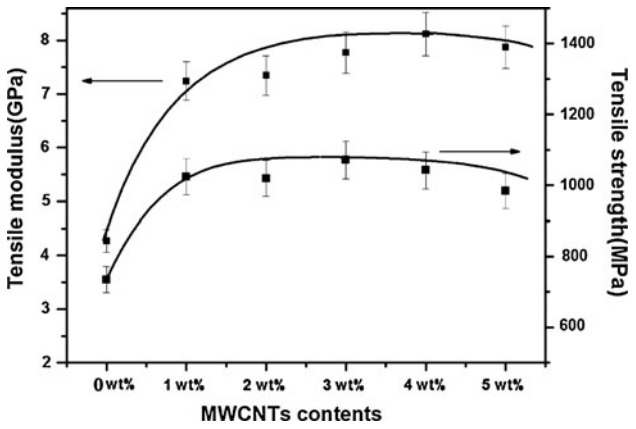

Fig. 7 Tensile properties of the neat PP and PP/MWCNTs nanocomposite fibers with 1–5 wt% MWCNTs

strength and modulus of composite fibers decreased at 5 wt% of MWCNTs. It was stated previously that the addition of 1 wt% MWCNTs into the PP matrix gave a significant increase in the percentage of crystallinity and 2–4 wt% MWCNTs provided a slight increase of this value but 5 wt% MWCNTs show the decrease in percentage of crystallinity, this corresponded well to the tensile property results. The crystalline part of materials has a major effect on the mechanical properties of the composites, as could be seen from the modulus improvement when the crystallinity increased. This was also reported by other researchers who studied on nanocomposite properties [13, 15, 32]. Table 3 compares the tensile modulus of this study to other researches. With the same content of MWCNTs (1 wt%), the percentage of modulus increase of this study is higher than Kearns's study. However, the modulus value of this work is lower due to the lower draw ratio.

Not only crystalline of the nanocomposite but also several factors improved the mechanical properties. It is well known that the reinforcement dispersion and alignment are important factors that could enhance the mechanical properties [44–46]. In addition, the interfacial adhesion between the reinforcement and matrix is also the significant issue [47, 48]. Figure 8a–c shows the SEM of 1, 3, and 5 wt% of the PP/MWCNTs nanocomposite fibers, while Fig 8d–f shows TEM images of the nanocomposite fibers. From the results of SEM and TEM images, it could be seen that for 1 and 3 wt% MWCNTs nanocomposite fibers, the dispersion of MWCNTs was better than that of 5 wt% MWCNTs nanocomposite fibers. It could be stated that the dispersion of the MWCNTS in the composite fibers related to both their tensile properties and crystallinity. A good dispersion provided a higher interfacial strength to give a more strength fibers. In addition, it could be concluded that both the amount of MWCNTs and their dispersion governed the crystallization of PP. Therefore, the 3 wt% MWCNTs nanocomposite fibers, which contained higher amount of MWCNTs than the 1 wt% MWCNTs and showed a good dispersion, imparted the highest crystallinity, while the add up of the amount of MWCNTs to 5 wt% could not further enhance the crystallinity of PP due to the MWCNTs agglomeration. Moreover, Fig. 8d–f revealed MWCNTs alignment along the fiber axis, which ultimately allowed the fillers to carry a larger amount of the applied load. Studies by Haggenmuller et al. [45, 49] have indeed demonstrated that the improved alignment of SWCNTs in PMMA and polyethylene fibers corresponded to the increase in nanocomposite modulus.

Conclusions

1. The crystallization temperature increased when the content of MWCNTs increased and the MWCNTs are nucleating agents in PP crystallization.
2. The crystallinity of PP matrix increased with the content of MWCNTs.
3. The XRD peak intensity of the nanocomposites showed the typical α-form PP crystals.

Table 3 The comparison of the modulus of the PP/CNTs nanocomposite fibers of this study to other researcher

Researchers	Fiber type	Draw ratios	wt% of CNTs	Modulus	
				GPa	% increase
Kearns and Shambaugh [16]	PP/MWCNTs	8.3	0	6.3	±0
			0.5	9.3	+47
			1	9.8	+55
Bhattacharyya et al. [8]	PP/SWCNTs	4.5	0	4.2	±0
			1	4.0	−4.8
This work	PP/MWCNTs	7.5	0	4.2	±0
			1	7.2	+69
			3	7.7	+81
			5	7.8	+84

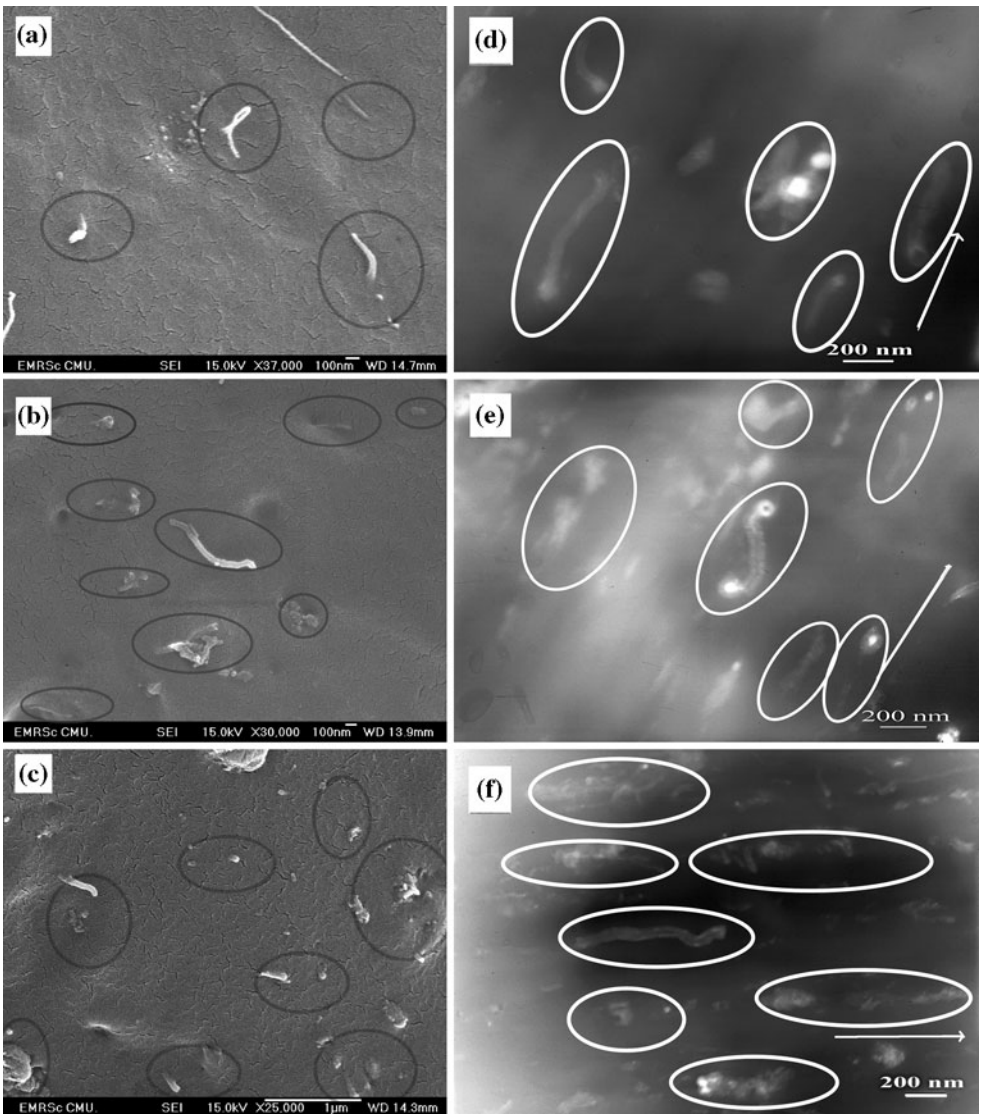

Fig. 8 The SEM images of **a** 1 wt%, **b** 3 wt%, **c** 5 wt% MWCNTs nanocomposite fibers and TEM images of **d** 1 wt%, **e** 3 wt%, **f** 5 wt% MWCNTs nanocomposite fibers

4. The onset of decomposition temperatures of nanocomposite fibers increased with the content of MWCNTs.
5. The tensile strength and modulus were significantly increased at 1 wt% MWCNTs of nanocomposite fibers and insignificantly increased with further increase of MWCNTs.
6. Good MWCNTs dispersion was found in low content of MWCNTs composites fibers (PP/1–4 wt% MWCNTs). However, the agglomeration was observed when high content of MWCNTs was loaded (PP/5 wt% MWCNTs).

Acknowledgements his work was supported by the NANOTEC, NSTDA, Ministry of Science and Technology, Thailand, through its program of Center of Excellence Network, the Higher Education Commission and Graduate School of Chiang Mai University.

References

1. Bethune DS, Klang CH, De Vries MS, Gorman G, Savoy R, Vazquez J, Beyers R (1993) Nature 363:605
2. Bandow S, Takizawa M, Hirahara K, Yudasaka M, Iijima S (2001) Chem Phys Lett 337:48
3. Baughman RH, Zakhidov AA, de Heer WA (2002) Science 297:787
4. Thess A, Lee R, Nikolaev P, Dai H, Petit P, Robert J, Xu C, Lee YH, Kim SG, Rinzler AG, Colbert DT, Scuseria GE, Tomanek D, Fischer JE, Smalley RE (1996) Science 273:483
5. Li YL, Kinloch IA, Windle AH (2004) Science 304:276
6. Zhang M, Atkinson KR, Baughman RH (2004) Science 306: 1358

7. Benoit JM, Corraze B, Chauvet O (2002) Phys Rev B 65:1405
8. Bhattacharyya AR, Sreekumar TV, Liu T, Kumar S, Ericson LM, Hauge RH, Smalley RE (2003) Polymer 44(8):2373
9. Mottaghitalab V, Xi B, Spinks GM, Wallace GG (2006) Synth Met 156:796
10. Sen R, Zhao B, Perea D, Itkis ME, Hu H, Love J, Bekyarova E, Haddon RC (2004) Nano Lett 4:459
11. Pecastaings G, Delhaes P, Derre A, Saadaoui H, Carmona F, Cui S (2004) J Nanosci Nanotech 4:838
12. Maier C, Calafut T (1998) Polypropylene: the definitive user's guide and databook. William Andrew Publishing, New York
13. Bao SP, Tjong SC (2008) Mater Sci Eng A 485:508
14. Hou Z, Wang K, Zhao P, Zhang Q, Yang C, Chen D, Du R, Fu Q (2008) Polymer 49:3582
15. Manchado MA, Valentini L, Biagiotti J, Kenny JM (2005) Carbon 43:1499
16. Kearns JC, Shambaugh RL (2002) J Appl Polym Sci 86:2079
17. Li C, Liang T, Lu W, Tang C, Hu X, Cao M, Liang J (2004) Compos Sci Technol 64:2089
18. Ganb M, Satapathy BK, Thunga M, Weidisch R, Potschke P, Jehnichen D (2008) Acta Mater 56:2247
19. Valentini L, Biagiotti J, Kenny JM, Santucci S (2003) Compos Sci Technol 63:1149
20. Seo MK, Lee JR, Park SJ (2005) Mater Sci Eng A 404:79
21. Wang L, Sheng J (2006) J Macro Sci B 45:1
22. Jose MV, Dean D, Tyner J, Price G, Nyairo G (2007) J Appl Polym Sci 103:3844
23. Kim JY, Han SI, Kim DK, Kim SH (2009) Compos Part A 40:45
24. Kashiwagi T, Grulke E, Hilding J, Harris R, Awad W, Douglas J (2002) Macromol Rapid Commun 23:761
25. Singjai P, Changsarn S, Thongtem S (2007) Mater Sci Eng A 443:42
26. Soitong T, Pumchusak J (2010) J Appl Polym Sci. http://onlinelibrary.wiley.com/doi/10.1002/app.32794/abstract
27. Young JA, Lovell PA (1991) Introduction to Polymer, 2nd edn. Stanley Thornes, Cornwall
28. Billmeyer FW (1984) Textbook of polymer science, 3rd edn. Wiley Interscience, New York
29. Revelen DWV (1976) Properties of polymers, 2nd edn. Elsevier Inc, New York
30. Brandrup J, Immergut EH (1989) Polymer handbooks, 3rd edn. Wiley Interscience, New York
31. Xu Z, Niu Y, Yang L, Xie W, Li H, Gan Z, Wang Z (2010) Polymer 51:730
32. Yang S, Tijerina JT, Diaz VS, Hernandez K, Lozano K (2007) Composite 38:228
33. Xiao C, Zhang Y, An S, Jia G (1996) J Appl Polym Sci 59:931
34. Yang BX, Shi JH, Pramoda KP, Goh SH (2008) Compos Sci Technol 68:2490
35. Li SN, Li ZM, Yang MB, Hu ZQ, Xu XB, Huang R (2004) Mater Lett 58:3967
36. Ma H, Zeng J, Realff ML, Kumar S, Schiraldi DA (2003) Compos Sci Technol 63:1617
37. Keith HD, Padden FJ, Vadimsky RG (1966) J Polym Sci 4:267
38. Li B, Hu GH, Cao GP, Liu T, Zhao L, Yuan WK (2008) J Supercrit Fluids 44:446
39. Wang Y, Cheng R, Liang L, Wang Y (2005) Compos Sci Technol 65:793
40. Chunyu L, Chou TW (2005) Mater Sci Eng A 409:140
41. Sheng Z, Horrocks AR (2003) J Polym Sci 28:1517
42. Philip J (2007) Plastics additives and compounding, May/June, 32–35
43. Lihua W, Jing S (2006) Macro Sci 45:1
44. Hasan MM, Zhou Y, Jeelani S (2007) Mater Lett 61:1134
45. Haggenmueller R, Gommans HH, Rinzler AG, Fischer JE, Winey KI (2000) Chem Phys Lett 330:219
46. Ward IM, Sweeney J (2004) The mechanical properties of solid polymer, 2nd edn. Wiley, England
47. Zhang Z, Zhang J, Chen P, Zhang B, He J, Hu GH (2006) Carbon 44:692
48. Zhou Z, Wang S, Lu L, Zhang Y, Znag Y (2008) Compos Sci Technol 68:1727
49. Haggenmueller R, Zhou W, Fischer JE, Winey KI (2003) J Nanosci Nanotechnol 3:105